



# A First-in-Human Phase 1 Study of a Tumor-Directed RNA-Interference Drug against HIF2 $\alpha$ in Patients with Advanced Clear Cell Renal Cell Carcinoma

James Brugarolas<sup>1</sup>, Gregory Obara<sup>2</sup>, Kathryn E. Beckermann<sup>3</sup>, Brian Rini<sup>3</sup>, Elaine T. Lam<sup>4</sup>, James Hamilton<sup>5</sup>, Thomas Schlupe<sup>5</sup>, Min Yi<sup>5</sup>, So Wong<sup>5</sup>, Zhongping Lily Mao<sup>5</sup>, Erick Gamelin<sup>6</sup>, and Nizar M. Tannir<sup>7</sup>

## ABSTRACT

**Purpose:** ARO-HIF2 is an siRNA drug designed to selectively target hypoxia-inducible factor-2 $\alpha$  (HIF2 $\alpha$ ) interrupting downstream pro-oncogenic signaling in clear cell renal cell carcinoma (ccRCC). The aims of this Phase 1 study (AROHIF21001) were to evaluate safety, tolerability, pharmacokinetics, and establish a recommended Phase 2 dose.

**Patients and Methods:** Subjects with ccRCC and progressive disease after at least 2 prior therapies that included VEGF and immune checkpoint inhibitors were progressively enrolled into dose-escalation cohorts of ARO-HIF2 administered intravenously at 225, 525, or 1,050 mg weekly.

**Results:** Twenty-six subjects received ARO-HIF2. The most common treatment emergent adverse events (AE) irrespective of causality were fatigue (50.0%), dizziness (26.9%), dyspnea (23.1%), and nausea (23.1%). Four subjects (15.4%) had treat-

ment-related serious AEs. AEs of special interest included neuropathy, hypoxia, and dyspnea. ARO-HIF2 was almost completely cleared from plasma circulation within 48 hours with minimal renal clearance. Reductions in HIF2 $\alpha$  were observed between pre- and post-dosing tumor biopsies, but the magnitude was quite variable. The objective response rate was 7.7% and the disease control rate was 38.5%. Responses were accompanied by ARO-HIF2 uptake in tumor cells, HIF2 $\alpha$  downregulation, as well as rapid suppression of tumor produced erythropoietin (EPO) in a patient with paraneoplastic polycythemia.

**Conclusions:** ARO-HIF2 downregulated HIF2 $\alpha$  in advanced ccRCC—inhibiting tumor growth in a subset of subjects. Further development was hampered by off-target neurotoxicity and low response rate. This study provides proof of concept that siRNA can target tumors in a specific manner.

## Introduction

The transcription factor hypoxia-inducible factor-2 $\alpha$  (HIF2 $\alpha$ ) is a key tumorigenic driver of clear cell renal cell carcinoma (ccRCC; refs. 1, 2). HIF2 $\alpha$  is a member of the HIF family of proteins, which also includes HIF1 $\alpha$  and HIF3 $\alpha$ . HIF $\alpha$  proteins dimerize with HIF1 $\beta$  (also called aryl hydrocarbon receptor nuclear translocator) and function as sequence-specific regulators of transcription. HIF $\alpha$  proteins are regulated by the von Hippel-Lindau (VHL) tumor-suppressor protein (pVHL; ref. 3). pVHL functions as the substrate recognition subunit of an E3 ubiquitin–ligase complex that promotes proteasome-mediated degradation of HIF $\alpha$ . VHL is frequently mutated in sporadic ccRCC, leading to constitutive HIF $\alpha$  accumulation (4, 5). VHL can also be

mutated in the germline, leading to ccRCC, hemangioblastomas, and paragangliomas in patients with VHL syndrome (1). Among the three known HIF $\alpha$  subunits, HIF2 $\alpha$  is believed to be the critical ccRCC driver (2, 3, 6–8).

The HIF2 complex promotes the expression of >100 genes (6, 9, 10), including VEGF, which binds to VEGF receptor-2 (VEGFR2) on endothelial cells to promote angiogenesis (11). ccRCC is characterized by high levels of VEGF (11), and multiple inhibitors of VEGF/VEGFR2 have been approved for the treatment of advanced ccRCC (12).

In addition to promoting angiogenesis, HIF2 $\alpha$  stimulates cell-cycle progression and maintains stemness, which likely contributes to tumorigenesis (13). Both Myc and E2F transcription factors have been shown to be induced by HIF2 $\alpha$  (6, 10, 14). Thus, inhibiting that HIF2 $\alpha$  would not only target the VHL/HIF/VEGF pathway more proximally, but also more broadly.

Although HIF2 $\alpha$  was considered “undruggable,” a structural vulnerability was identified (15). Subsequently, the small-molecule inhibitors PT2385, PT2399, and PT2977 were developed and showed activity in preclinical models of ccRCC (16–19). In addition, PT2385 and PT2977 demonstrated promising early activity in advanced ccRCC (20, 21). PT2977 (belzutifan) is FDA approved for patients with VHL disease (22) and was recently approved for patients with advanced ccRCC. Thus, HIF2 $\alpha$  is a validated therapeutic target. However, resistance mutations occur with prolonged treatment (16, 23) highlighting the need for complementary therapeutic approaches.

siRNAs are an emerging, highly specific treatment modality. ARO-HIF2 (zifcasiran) is an siRNA synthetic double-stranded RNAi trigger. RNAi is a naturally occurring catalytic gene silencing mechanism that is highly specific and efficient (24, 25). ARO-HIF2 engages the cell's RNAi machinery to target HIF2 $\alpha$  (EPAS1) mRNA for degradation, thereby reducing the amount of free HIF2 $\alpha$  mRNA available for

<sup>1</sup>The University of Texas Southwestern Medical Center, Dallas, Texas. <sup>2</sup>Comprehensive Cancer Centers of Nevada, Henderson, Nevada. <sup>3</sup>Vanderbilt-Ingram Cancer Center, Nashville, Tennessee. <sup>4</sup>University of Colorado Cancer Center, Anschutz Medical Campus, Aurora, Colorado. <sup>5</sup>Arrowhead Pharmaceuticals, Pasadena, California. <sup>6</sup>Gamelin Biopharma Consulting, Wilmington, Delaware. <sup>7</sup>The University of Texas MD Anderson Cancer Center, Houston, Texas.

**Corresponding Authors:** James Brugarolas, UT Southwestern Medical Center, 5323 Harry Hines Boulevard, Dallas, TX 75390-9133. E-mail: james.brugarolas@utsouthwestern.edu; and Nizar M. Tannir, The University of Texas MD Anderson Cancer Center, Department of Genitourinary Medical Oncology, 1515 Holcombe Blvd, Unit 1374, Houston, TX 77030. E-mail: ntannir@mdanderson.org

Clin Cancer Res 2024;XX:XX–XX

doi: 10.1158/1078-0432.CCR-23-3029

This open access article is distributed under the Creative Commons Attribution-NonCommercial-NoDerivatives 4.0 International (CC BY-NC-ND 4.0) license.

©2024 The Authors; Published by the American Association for Cancer Research

## Translational Relevance

siRNAs are a highly specific treatment modality under development for multiple indications. Here, we report the results of a Phase 1 clinical study of ARO-HIF2, a tumor-directed siRNA against HIF2 $\alpha$ , a key driver of clear cell renal cell carcinoma (ccRCC). This study reports on safety, pharmacokinetics and tumor distribution, activity, and pharmacodynamic measures of target engagement. Overall, the study provides proof of concept for tumor-directed oligonucleotide-based therapies in oncology.

translation. This lowers the amount of HIF2 $\alpha$  protein available to dimerize with HIF1 $\beta$ , interrupting downstream pro-oncogenic gene activation.

In metastatic ccRCC,  $\alpha$ v $\beta$ 3 ( $\alpha$ v $\beta$ 3) integrin receptors are often overexpressed (26, 27). ARO-HIF2 is conjugated to a small-molecule ligand for  $\alpha$ v $\beta$ 3, which directs ARO-HIF2 to tumor cells and promotes efficient cellular uptake. The targeting strategy was developed using human A498 ccRCC cells injected orthotopically into nude mice (28). Conjugated to an  $\alpha$ v $\beta$ 3-targeting ligand, the HIF2 $\alpha$  siRNA was efficiently taken up by tumor cells leading to robust knockdown whilst untargeted siRNA showed minimal uptake and knockdown (29). Although  $\alpha$ v $\beta$ 3 is expressed beyond ccRCC, the targeting strategy relies on ligand-mediated uptake in ccRCC cells, the high specificity of the siRNA, and the observation that broader HIF2 $\alpha$  inhibition with small molecules has low toxicity.

HIF2 $\alpha$  siRNA drugs showed promise in preclinical tumor models. A first-generation siRNA drug was taken up by ccRCC cell lines leading to HIF2 $\alpha$  knockdown, and a correlation was observed between the magnitude of knockdown and tumor growth inhibition in xenografts (28, 29). The same siRNA drug was taken up by patient-derived ccRCC tumorgrafts expressing  $\alpha$ v $\beta$ 3, where it reduced HIF2 $\alpha$  levels, downregulated HIF2 target genes, including VEGF, and led to substantial anti-tumor activity (10). In these tumorgraft models, the siRNA drug exhibited comparable activity with PT2399. Notably, the siRNA drug effectively depletes not only wild-type HIF2 $\alpha$ , but also resistant mutant HIF2 $\alpha$  (10). The same tumorgraft models were evaluated using a second-generation siRNA drug, ARO-HIF2, which targets the same HIF2 $\alpha$  mRNA sequence but is more easily manufactured. ARO-HIF2 was similarly taken up by ccRCC tumorgrafts but was not quite as potent as the first-generation inhibitor (10).

The aims of this Phase 1 dose-finding study (AROHIF21001) were to evaluate the safety, tolerability, and pharmacokinetics (PK) of ARO-HIF2, and to establish a recommended Phase 2 dose (RP2D) based on preliminary efficacy and pharmacodynamic effects in patients with advanced ccRCC.

## Patients and Methods

### Study design

AROHIF21001 (NCT04169711) was a multicenter, open-label, dose-finding clinical study of ARO-HIF2, administered intravenously in patients with advanced ccRCC. The screening period was up to 28 days, the maximum duration permitted on study treatment was 2 years, and post-study follow-up comprised monthly contact for 6 months.

The primary objectives were to assess the safety and tolerability of ARO-HIF2 and to determine the RP2D based on safety, preliminary efficacy, and pharmacodynamic effect. The secondary objectives

included PK evaluation of ARO-HIF2, and preliminary efficacy based on RECIST Version 1.1. Exploratory objectives included analyses of HIF2 $\alpha$  gene and protein expression. Other relevant proteins pertaining to ARO-HIF2 treatment and response (VEGF; erythropoietin, EPO) were also evaluated.

The study was conducted in accordance with the principles of the Declaration of Helsinki, the International Council for Harmonization Good Clinical Practice guidelines, and applicable regulatory requirements, including Institutional Review Board (IRB) approval. All subjects provided written informed consent before enrollment.

### Participants

Up to 50 subjects (including replacements) were expected to be enrolled in up to 5 cohorts (6 subjects per cohort; Supplementary Fig. S1). Up to an additional 4 subjects per cohort could be enrolled to ensure at least 4 complete sets of paired (pre- and post-dose) viable tumor biopsy samples.

Eligible subjects were  $\geq$ 18 years of age with histologically confirmed, locally advanced or metastatic ccRCC, whose disease had progressed during treatment with or otherwise failed at least 2 prior approved therapeutic regimens for ccRCC, including VEGF-targeted therapy and immune checkpoint inhibitor (ICI) therapy. All subjects were required to have Eastern Cooperative Oncology Group (ECOG) performance status 0–1, adequate organ function, and an estimated life expectancy  $>$ 3 months.

The main exclusion criteria were untreated brain metastasis, leptomeningeal disease or spinal cord compression, history of solid organ or stem cell transplantation, use of VEGF/mTOR/immune checkpoint inhibitors within 2 weeks before first dose, and failure to recover (to Grade  $\leq$ 1) from the effects of prior anticancer therapy. A full list of inclusion and exclusion criteria is provided in the Supplement.

### Treatment and dose escalation

ARO-HIF2 was administered by intravenous infusion at 225 mg weekly (QW; Cohort 1), 525 mg QW (Cohort 2), and 1,050 mg QW (Cohort 3) for up to 2 years (Supplementary Fig. S1).

Dose-limiting toxicities (DLT) were evaluated for each subject during the first 28 days from the initial dose of ARO-HIF2. A DLT was defined as an AE Grade  $\geq$ 3 assessed as at least probably related to ARO-HIF2 by the Investigator. Safety was monitored on an ongoing basis. Cumulative safety data (e.g., AEs, laboratories, vital signs) were evaluated by the Data Review Committee before dose escalation to the next cohort (Supplementary Fig. S1). If no DLTs were reported through the DLT window, screening could begin for the next planned cohort. Subjects were replaced if they withdrew from the study before clearing the 28-day DLT window with fewer than 3 ARO-HIF2 doses for reasons other than an AE considered at least possibly related to ARO-HIF2 or if they did not undergo the first post-treatment biopsy.

### Safety and efficacy assessments

The safety of ARO-HIF2 was evaluated on the basis of the following assessments: monitoring of AEs/serious adverse events (SAE), infusion reactions, vital signs, physical exam, clinical laboratory tests (including pregnancy tests in females of childbearing potential), electrocardiogram measurements, concomitant medications/therapy, and reasons for treatment discontinuation due to toxicity. AEs were evaluated using NCI Common Terminology Criteria for AEs v5.0.

RECIST v1.1 was used to evaluate target lesions using CT or MRI. Lesions were evaluated every 8 weeks (Q8W) after the first dose. Assessments were made by the Investigators without confirmatory scans.

### Pharmacokinetics

Blood and urine samples were collected for PK and metabolite analyses. Samples for plasma PK analysis were collected pre-dose, 15, 30 minutes, 1, 2, 4, 24, and 48 hours post-dose during week 1, 3, and in some subjects during week 4. Urine samples were collected pre-dose and at 24 hours post-dose. PK analyses were performed using actual collection times. A noncompartmental analysis of ARO-HIF2 plasma levels was conducted on the basis of concentration-time profiles of the full-length anti-sense strand using a good laboratory practice-validated sequence-specific peptide nucleic acid fluorescence hybridization assay using anion-exchange high performance liquid chromatography coupled with fluorescence detection (30). Parameters included AUC from 0 to 24 hours ( $AUC_{0-24}$ ), AUC from 0 to the time of the last observed concentration ( $AUC_{all}$ ), maximum concentration ( $C_{max}$ ), time to reach maximum plasma concentration ( $T_{max}$ ), volume of distribution at steady state ( $V_{ss}$ ), systemic clearance (CL), amount of drug excreted in the urine over one dosing interval through 24 hours post-dose ( $Ae_{0-24}$ ), fraction excreted in the urine ( $fe_{0-24}$ ), and renal clearance calculated by  $Ae_{0-24h}/AUC_{0-24h}$  ( $CL_R$ ).

### Tumor biopsy collection and processing

Core needle biopsies were collected from the same lesions at baseline and at 2 weeks. A third tumor biopsy sample collection at the end-of-study was optional. Tissue was collected by performing 2 to 5 biopsy passes using a 14- to 18-gauge needle under CT or ultrasound guidance. Core biopsies to be submitted were formalin-fixed and incorporated into a single paraffin embedded (FFPE) block using standard institutional procedures. Blocks were cut into 5- $\mu$ m sections and mounted on white Superfrost Positive Plus slides. One slide was stained for hematoxylin and eosin (H&E) and submitted for pathologist review to confirm ccRCC consistent with the primary diagnosis and to determine tumor cell content.

### RT-qPCR for *HIF1 $\alpha$* and *HIF2 $\alpha$* mRNA expression

The *HIF1 $\alpha$*  and *HIF2 $\alpha$*  RT-qPCR assay is a 1-step triplex assay composed of primer/probe sets that target *HIF1 $\alpha$*  and *HIF2 $\alpha$*  as well as the reference gene importin 8 (*IPO8*). The *HIF1 $\alpha$*  assay amplifies a 76bp region spanning exon 4/exon 5 of the *HIF1 $\alpha$*  gene whereas the *HIF2 $\alpha$*  assay amplifies a 68bp region spanning exon 7/8. A commercially available assay was used for *IPO8* (*IPO8* TaqMan Gene Expression assay, Thermo Fisher Scientific). A minimum tumor content of 40% tumor cells as assessed by a pathologist on an H&E slide of the tissue section was required. If the tissue had less than 40% tumor content, microdissection was performed to isolate an area of the tissue with >40% tumor content, if possible. If no area with >40% tumor content could be isolated, the sample was not analyzed and reported as tumor content not sufficient. A minimum of 4 FFPE sections were used for RNA extraction using a Maxwell CSC RNA FFPE Kit on a Promega Maxwell CSC instrument (Promega). RNA concentration was determined by NanoDrop 2000c spectrophotometer (Thermo Fisher Scientific). A mass input of 10-ng RNA per 20  $\mu$ L RT-qPCR reaction was used. Amplification was performed by reverse transcription at 48°C for 15 minutes, enzyme activation at 95°C for 10 minutes followed by up to 40 cycles of denaturation at 95°C for 15 seconds and annealing/extension at 60°C for 60 seconds in triplicate. Data analysis was performed by using average  $C_t$  values.  $\Delta\Delta C_t$  and percentage of change (% change) were calculated using the following formulas:

$$\Delta\Delta C_t = ABS(\Delta C_t \text{ post-treatment} - \Delta C_t \text{ pre-treatment})$$

$$\% \text{ change} = 100 - ([2^{-\Delta\Delta C_t}] * 100)$$

The assay has a linear  $C_t$  range of 26.9 to 38, corresponding to approximately 20 to 0.0049 ng RNA input.

### Immunohistochemical detection and quantification of HIF2 $\alpha$ protein

Slides were stained on a Leica Bond III immunostainer (Leica). A minimum tumor content of 5% was required. Briefly, FFPE sections were deparaffinized, subjected to high temperature epitope retrieval, quenched with endogenous peroxidase blocker, treated with background stain blocking agent (10% normal goat serum), and washed before application of primary antibody. For HIF2 $\alpha$ , the primary antibody was a rabbit mAb (clone 2444A, Novus Biologicals/Thermo Fisher Scientific) diluted in Leica Bond Antibody Diluent to a final concentration of 10.0  $\mu$ g/mL. For  $\alpha$ v $\beta$ 3 the primary antibody was a rabbit mAb (Clone D7 $\times$ 3P, Cell Signaling Technology) diluted in Leica Bond Antibody diluent to a final concentration of 1.0  $\mu$ g/mL. Detection of the bound primary antibody was achieved using the Bond Polymer Refine kit 3,3' diaminobenzidine chromogen for visualization. Slides were counterstained with hematoxylin to label nuclei, and cover slipped using permanent mounting medium. Predominant nuclear HIF2 $\alpha$  staining intensity was reported as 0, 1+, 2+, or 3+ in tumor cells. The percentage of positively stained tumor cells at each staining intensity was reported as 0% to 100%. H-score was calculated as follows: H-score = 3\*(% tumor at 3+ intensity) + 2\*(% tumor at 2+ intensity) + 1\*(% tumor at 1+ intensity).

### ISH for *HIF2 $\alpha$* mRNA detection and quantification

FFPE tissue sections were pretreated using standard RNAscope (Advanced Cell Diagnostics, ACD) processes. Briefly, slides were baked in a dry oven for 1 hour at 60°C, deparaffinized for approximately 20 minutes, and then subjected to epitope retrieval for 15 minutes at 95°C, and protease III treatment for 15 minutes at 40°C. ISH of the probe for *HIF2 $\alpha$*  (ACD RNAscope LS 2.5 Probe-HS-EPAS1, catalog No. 410598) and signal amplification was performed using standard conditions. Slides were counterstained with H&E and analyzed by HALO image analysis software (Indica Labs) in two regions, tumor ( $\geq$ 100 cells) and non-tumor. Cells were grouped into 5 bins (scoring categories), with bin 0 having 0 dots/cell, bin 1 having 1 to 3 dots per cell, bin 2 having 4 to 9 dots per cell, bin 3 having 10 to 15 dots per cell, and bin 4 having >15 dots per cell. H-score was calculated as follows: H-score = 4\*(% cells at bin 4) + 3\*(% cells at bin 3) + 2\*(% cells at bin 2) + 1\*(% cells at bin 1).

### ISH for ARO-HIF2 trigger detection and quantification

FFPE tissue sections were pretreated using standard miRNAscope (ACD) LS Reagent Kit-RED processes with the following modifications: Extended offline baking was performed for 60 minutes at 60°C, xylene dewaxing was extended to 4  $\times$  10 minutes, and 100% ethanol dehydration was performed for 3  $\times$  2 minutes. Standard processes were used for epitope retrieval (15 minutes at 95°C) and protease III treatment (15 minutes at 40°C). ISH was performed with a custom probe complementary to the ARO-HIF2 trigger sequence and signal amplification was performed using standard conditions. Slides were counterstained with H&E and analyzed by HALO image analysis software (Indica Labs) in two regions, tumor and non-tumor (stroma). Cells were grouped into 4 bins (scoring categories), with bin 0 having 0 dots/cell, bin 1 having 1 to 10 dots per cell, bin 2 having 11 to 20 dots per cell, and bin 3 having >20 dots per cell. H-score was calculated as follows: H-score = 3\*(% cells at bin 3) + 2\*(% cells at bin 2) + 1\*(% cells at bin 1).

### *VHL* mutation detection by NGS

A minimum of 5 FFPE slides were used to extract DNA using RecoverALL Total Nucleic Acid Isolation Kit for FFPE (Thermo Fisher

Scientific). DNA concentration was determined using Qubit and Nanodrop. A minimum of 100 ng of DNA was required. The ArcherDx VariantPlex Solid Tumor Panel NGS assay performed according to the manufacturer's instructions was used to evaluate *VHL* mutations. Illumina MiSeq was used as the sequencing platform. Proprietary bioinformatics analysis was performed by MolecularMD (a subsidiary of ICON Clinical Research).

### Statistical analysis

Safety and efficacy analyses included subjects who received at least one dose of ARO-HIF2 (Safety Analysis Set). Treatment emergent AEs (TEAE) were summarized by System Organ Class and Preferred Term using Medical Dictionary for Regulatory Activities v22.1. The incidence of AEs, SAEs, and AEs leading to withdrawal, dose modification, or treatment discontinuation were summarized. PK parameters were determined using noncompartmental methods. Descriptive statistics of PK parameters include mean, standard deviation, coefficient of variation, median, and range. Best overall response (BOR) for a subject was the best observed disease response per RECIST v1.1. Responses [complete response (CR) + partial response (PR)] were based on an assessment by the Investigator and no confirmation was needed. Objective response rate (ORR) was defined as the proportion of subjects with a BOR of CR or PR. ORR and corresponding 95% confidence intervals were derived. Disease control rate (DCR) was defined as the proportion of subjects whose BOR was determined as CR, PR, or stable disease (SD; assessed Q8W until week 56).

### Data availability statement

Subject to privacy, ethical, informed consent, and other similar legal restrictions, the data generated in this study are available upon reasonable request directed to the corresponding authors.

## Results

Twenty-six subjects enrolled in the study: 7 subjects in Cohort 1 (225 mg QW), 10 subjects in Cohort 2 (525 mg QW), and 9 subjects in Cohort 3 (1,050 mg QW; **Table 1**; Supplementary Figs. S1 and S2).

### Demographics, baseline characteristics, and disease history

Most subjects were male (76.9%) and White (88.5%), with a median age of 67.5 years (range, 44, 87; **Table 1**). The median time from metastatic diagnosis to enrollment was 37.8 months (range, 4.6–173.9). All subjects had histologically confirmed ccRCC and ECOG performance score of 0–1; 53.8% of subjects had International Metastatic RCC Database Consortium intermediate-risk, 23.1% had good-risk, and 15.4% had poor-risk disease. All subjects received at least 2 prior lines of therapy, including VEGF-directed therapy and ICI therapy. The number of prior lines of therapy were 2 (26.9%), 3 (34.6%), and  $\geq 4$  (38.5%). Overall, 19 of 26 subjects had valid NGS data for *VHL* in tumor samples, of which 15 subjects (78.9%) had an intragenic or splice site mutation (**Table 1**).

### Safety profile

TEAEs occurred in 96.2% of subjects and the most common TEAEs of any grade irrespective of causality were fatigue (50.0%), dizziness (26.9%), dyspnea and nausea (23.1% each), constipation (19.2%), as well as headache and muscle weakness (15.4% each; **Table 2**). Grade  $\geq 3$  TEAEs were reported in 38.5% of subjects.

Treatment-related Grade  $\geq 3$  TEAEs were reported in 15.4% of subjects (Cohorts 2 and 3) and included blood creatinine increase,

encephalopathy, hypoxia, and peripheral neuropathy. Neuropathy was determined to be an AE of special interest (AESI) and included the preferred terms of chronic inflammatory demyelinating polyradiculoneuropathy (CIDP), demyelinating polyneuropathy, neuropathy peripheral, and peripheral sensory neuropathy. Six subjects (23.1%) had treatment emergent neuropathic AESIs related to ARO-HIF2 (8 events; Supplementary Table S1) including a Grade 4 peripheral neuropathy (not recovered/not resolved). These do not include two additional events, a Grade 3 CIDP (not recovered/not resolved) and a Grade 3 Guillain–Barre syndrome (recovered/resolved), that were reported after study discontinuation. A sural nerve biopsy was performed on one subject that experienced Grade 3 CIDP. Histological analysis showed findings typical of diabetic neuropathy and the subject was previously diagnosed with type 2 diabetes. H&E and HIF2 trigger (miRNAscope) stains showed ARO-HIF2 in microvasculature around the nerve but limited staining in the nerve sheath. Although neurological symptoms persisted throughout the study window, approximately 10 months after the CIDP diagnosis, the subject had a remarkable recovery of neurological function to baseline. Treatment-related AESIs of dyspnea and hypoxia were reported in 15.4% and 7.7% of subjects, respectively (Supplementary Table S1).

SAEs were reported in 34.6% of subjects (18 events). Treatment related SAEs were reported in 15.4% of subjects (5 events). No protocol-defined DLTs were reported in any of the 3 dose escalation cohorts. TEAEs leading to study drug held or withdrawal were reported in 10 subjects (38.5%); however, no preferred terms were reported in  $>1$  subject. One fatal TEAE of Grade 5 acute respiratory failure was attributed to disease progression and not related to ARO-HIF2.

All 26 subjects discontinued the study (Supplementary Fig. S2). The most common reasons were disease progression/symptomatic deterioration (73.1%) and AE or laboratory abnormality (15.4%).

### PK profile

ARO-HIF2 was almost completely cleared from plasma circulation within 48 hours across dose levels (Supplementary Tables S2 and S3, Supplementary Fig. S3). The systemic distribution of ARO-HIF2 appeared to be restricted to plasma volume (approximately 3L). Mean systemic clearance was 0.3 to 1.4 L/h and renal clearance was minimal (Supplementary Tables S2 and S4). Marked PK nonlinearity was observed that could have been due to rate-limited endocytosis based on receptor capacity. Although the  $C_{max}$  and AUC increased with dose, ARO-HIF2 did not show accumulation in plasma with repeat QW dosing. The inter-subject PK variability for the 3 cohorts was moderate to high with geometric mean coefficient of variation (CV%) up to 50% for  $AUC_{0-24}$  and up to 35% for  $C_{max}$ .

ARO-HIF2 distribution to tumor tissue showed a dose dependent increase in siRNA trigger concentrations in tumor cells (Supplementary Table S5 and Supplementary Fig. S4). Median tumor cell concentration increased with dose in a non-linear fashion with H-scores of 108, 215, and 254 at 225 mg, 525 mg, and 1,050 mg, respectively. Cellular concentration in stromal cells was largely constant across all dose levels (median H-score of 241 to 257) and similar to the concentration observed in tumor cells at the highest dose level of ARO-HIF2.

### Tumor response

Of the 26 subjects, 2 subjects (7.7% of total cohort) had BOR of PR, 8 subjects (30.8%) had SD at week 8, and 14 subjects (53.8%) had progressive disease (**Table 3**, **Figs. 1 and 2**). Of the 8 subjects with

**Table 1.** Demographics and baseline disease characteristics.

Characteristic	ARO-HIF2 225 mg (N = 7)	ARO-HIF2 525 mg (N = 10)	ARO-HIF2 1,050 mg (N = 9)	Total (N = 26)
Median Age (y; range)	72.0 (55–75)	68.0 (63–87)	59.0 (44–74)	67.5 (44–87)
Sex, n (%)				
Male, n (%)	6 (85.7)	7 (70.0)	7 (77.8)	20 (76.9)
Female, n (%)	1 (14.3)	3 (30.0)	2 (22.2)	6 (23.1)
Race, n (%)				
White	7 (100.0)	9 (90.0)	7 (77.8)	23 (88.5)
Other	0	1 (10.0)	1 (11.1)	2 (7.7)
Multiple	0	0	1 (11.1)	1 (3.8)
Median BMI (kg/m <sup>2</sup> ; range)	24.4 (20.7–31.5)	26.5 (17.4–33.0)	25.7 (20.2–37.2)	25.5 (17.4–37.2)
IMDC Criteria, n (%)				
Good Risk	1 (14.3)	4 (40.0)	1 (11.1)	6 (23.1)
Intermediate Risk	5 (71.4)	5 (50.0)	4 (44.4)	14 (53.8)
Poor Risk	1 (14.3)	1 (10.0)	2 (22.2)	4 (15.4)
Missing	0	0	2 (22.2)	2 (7.7)
ECOG Performance Status, n (%)				
0	4 (57.1)	4 (40.0)	3 (33.3)	11 (42.3)
1	3 (42.9)	6 (60.0)	6 (66.7)	15 (57.7)
Time from metastatic disease to enrollment (mo)				
Median (range)	38.5 (5.3–96.6)	39.8 (20.9–112.4)	37.1 (4.6–173.9)	37.8 (4.6–173.9)
Number of prior lines of cancer therapy, n (%)				
1	0	0	0	0
2	2 (28.6)	3 (30.0)	2 (22.2)	7 (26.9)
3	2 (28.6)	4 (40.0)	3 (33.3)	9 (34.6)
≥4	3 (42.9)	3 (30.0)	4 (44.4)	10 (38.5)
Prior therapy for renal cancer, n (%)				
ICI	7 (100.0)	10 (100.0)	9 (100.0)	26 (100.0)
VEGF-Directed Therapy	7 (100.0)	10 (100.0)	9 (100.0)	26 (100.0)
mTOR Inhibitor	2 (28.6)	3 (30.0)	2 (22.2)	7 (26.9)
Non-ICI Immunotherapy	2 (28.6)	0	3 (33.3)	5 (19.2)
Targeted therapy (other) <sup>a</sup>	2 (28.6)	0 (0.0)	0	2 (7.7)
Biologic therapy <sup>a</sup>	1 (14.3)	0	0	1 (3.8)
Chemotherapy <sup>b</sup>	1 (14.3)	0	0	1 (3.8)
HIF2 Inhibitor	0	0	0	0
VHL Mutation Status by NGS, n (%) <sup>c</sup>				
Frameshift	2 (28.6)	1 (10.0)	2 (22.2)	5 (19.2)
Missense variant	1 (14.3)	4 (40.0) <sup>d</sup>	2 (22.2)	7 (26.9) <sup>d</sup>
In-frame-deletion	0	1 (10.0)	0	1 (3.8)
Splice site	0	0	1 (11.1)	1 (3.8)
Stop gained	0	1 (10.0) <sup>d</sup>	1 (11.1)	2 (7.7) <sup>d</sup>
No mutation detected	2 (28.6)	0	2 (22.2)	4 (15.4)
Not available	2 (28.6)	4 (40.0)	1 (11.1)	7 (26.9)

Abbreviations: BMI, body mass index; ECOG, Eastern Cooperative Oncology Group; HIF2, hypoxia-inducible factor-2; ICI, immune checkpoint inhibitor; IMDC, International Metastatic RCC Database Consortium; mTOR, mammalian target of rapamycin; N, total number of subjects; n, subject incidence; NGS, next-generation sequencing; VEGF, vascular endothelial growth factor; VHL, von Hippel-Lindau gene.

<sup>a</sup>Experimental therapy.

<sup>b</sup>Tenth line 5FU and gemcitabine.

<sup>c</sup>From screening samples except when not evaluable or not available, when results from the next available suitable biopsy are shown.

<sup>d</sup>In one subject, the same tumor had both a missense variant and a stop codon gain.

SD at Week 8, 4 subjects (15.4%) had SD at Week 16 (**Fig. 1**). Across all cohorts, ORR was 7.7% (95% CI, 0.9–25.1; 0 CR–2 PR) and DCR was 38.5% (95% CI, 20.2–59.4; **Table 3**).

The median number of weekly infusions was 8.0 (range, 2–48; Supplementary Table S6). The median duration of exposure was comparable in Cohort 1 (225 mg, 8.0 weeks) and 3 (1,050 mg, 8.1 weeks), but was higher in Cohort 2 (525 mg, 11.2 weeks). The mean (standard deviation) relative dose intensity was well maintained between dose levels: Cohort 1 (98.0%; 5.4), Cohort 2 (92.6%; 7.6), and Cohort 3 (93.3%; 10.9). Overall, the mean relative dose intensity was 94.3% (8.4).

### Pharmacodynamic profile

Reduced HIF2 $\alpha$  mRNA by ISH was observed in 13 of 19 subjects, with 3.9%, 26.4%, and 22.4% median reduction from baseline in Cohorts 1 to 3, respectively. All 9 subjects with evaluable biopsies for HIF2 $\alpha$  mRNA by RT-qPCR had reduced levels with 46%, 23%, and 44% median reductions from baseline in Cohorts 1 to 3, respectively. Reduced HIF2 $\alpha$  protein by IHC was observed in 9 of 14 evaluable subjects, with 27% and 47% median reductions from baseline in Cohorts 1 and 2, respectively. Unexpectedly, the median change in HIF2 $\alpha$  protein by IHC from baseline in Cohort 3 was 0. Overall, reductions in tumor HIF2 $\alpha$  mRNA and protein were highly variable.

**Table 2.** Summary of treatment emergent adverse events (safety analysis set).

Subject incidence, n (%)	ARO-HIF2 225 mg (N = 7)	ARO-HIF2 525 mg (N = 10)	ARO-HIF2 1,050 mg (N = 9)	Total (N = 26)
TEAEs	7 (100.0)	10 (100.0)	8 (88.9)	25 (96.2)
TEAEs by severity <sup>a,b</sup>				
Grade 1	2 (28.6)	3 (30.0)	2 (22.2)	7 (26.9)
Grade 2	3 (42.9)	3 (30.0)	2 (22.2)	8 (30.8)
Grade 3	1 (14.3)	3 (30.0)	4 (44.4)	8 (30.8)
Grade 4	0	1 (10.0)	0	1 (3.8)
Grade 5	1 (14.3)	0	0	1 (3.8)
Treatment-related TEAEs	5 (71.4)	7 (70.0)	5 (55.6)	17 (65.4)
Treatment-related TEAEs grade $\geq 3^a$	0	2 (20.0)	2 (22.2)	4 (15.4)
Treatment emergent SAE	2 (28.6)	4 (40.0)	3 (33.3)	9 (34.6)
Treatment-related SAE	0	3 (30.0)	1 (11.1)	4 (15.4)
TEAEs leading to study drug held or withdrawal	2 (28.6)	4 (40.0)	4 (44.4)	10 (38.5)
TEAEs by preferred term occurring in $>3$ subjects				
Fatigue	5 (71.4)	5 (50.0)	3 (33.3)	13 (50.0)
Dizziness	1 (14.3)	4 (40.0)	2 (22.2)	7 (26.9)
Dyspnea	1 (14.3)	2 (20.0)	3 (33.3)	6 (23.1)
Nausea	1 (14.3)	3 (30.0)	2 (22.2)	6 (23.1)
Constipation	0	2 (20.0)	3 (33.3)	5 (19.2)
Headache	0	3 (30.0)	1 (11.1)	4 (15.4)
Muscular weakness	0	3 (30.0)	1 (11.1)	4 (15.4)

Note: The safety analysis set included all enrolled subjects who received at least 1 dose of study drug.

Abbreviations: N, total number of subjects; SAE, serious adverse event; TEAE, treatment emergent adverse event.

<sup>a</sup>The severity of each adverse event was graded using Common Terminology Criteria for Adverse Events (CTCAE) version 5.0.

<sup>b</sup>A subject with 2 or more TEAEs within a preferred term was counted only once at the highest CTCAE grade.

In the two subjects with a PR, HIF2 $\alpha$  mRNA was reduced by 33% and 36%, respectively (Table 4).

HIF1 $\alpha$  mRNA was measured to evaluate the specificity of ARO-HIF2. No substantial change in HIF1 $\alpha$  mRNA from baseline was observed in pre- and post-treatment biopsies by RT-qPCR (median percentage of change  $<5\%$ ).

Erythropoietin (EPO), a well-established HIF2 $\alpha$  target gene, is normally produced by kidney cells, but can also be produced by ccRCC. It is unclear whether ARO-HIF2 is taken up by normal EPO-producing cells. There were no mean changes in EPO in Cohort

1. However, there was a reduction in EPO at the higher dose levels, but no subjects had reductions in EPO levels below the normal threshold of 2.6 IU/L (Supplementary Fig. S5). In a subject with paraneoplastic polycythemia with baseline levels approximately 200 IU/L, a profound downregulation in EPO was observed (10).

Decreases in hemoglobin were observed with maximum mean reductions from baseline over time of 7.9% (week 4,  $n = 5$ ), 20.6% (week 15,  $n = 5$ ), and 12.8% (week 7,  $n = 6$ ; Supplementary Fig. S6).

We also evaluated VEGF levels. No reductions in mean VEGF levels were observed (Supplementary Fig. S7).

**Table 3.** Summary of efficacy.

Subject incidence, n (%)	ARO-HIF2 225 mg (N = 7)	ARO-HIF2 525 mg (N = 10)	ARO-HIF2 1,050 mg (N = 9)	Total (N = 26)
Best overall response RECIST <sup>a</sup>				
Complete response (CR)	0	0	0	0
Partial response (PR)	0	1 (10.0)	1 (11.1)	2 (7.7)
Stable disease (SD) <sup>b</sup>	1 (14.3)	5 (50.0)	12 (22.2)	8 (30.8)
Progressive disease (PD)	5 (71.4)	3 (30.0)	6 (66.7)	14 (53.8)
Not evaluable	0	0	0	0
Not available	1 (14.3)	1 (10.0)	0	2 (7.7)
Objective response rate (CR+PR)	0	1 (10.0)	1 (11.1)	2 (7.7)
95% CI	0–41.0	0.3–44.5	0.3–48.2	0.9–25.1
Disease control rate (CR+PR+SD)	1 (14.3)	6 (60.0)	3 (33.3)	10 (38.5)
95% CI	0.4–57.9	26.2–87.8	7.5–70.1	20.2–59.4

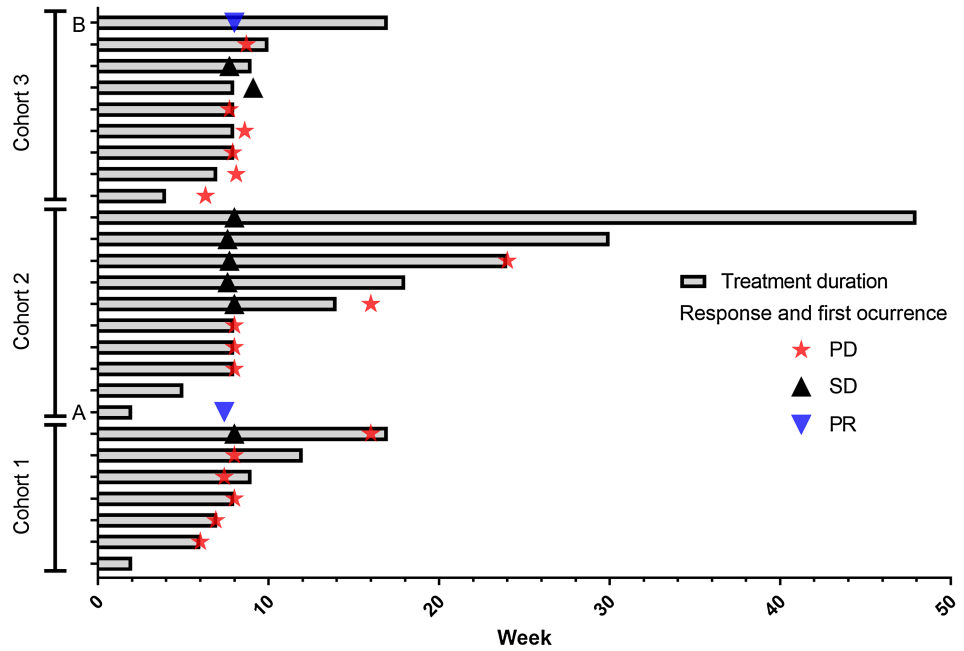
Abbreviations: CI, confidence interval; N, total number of subjects; RECIST, response evaluation criteria in solid tumors.

<sup>a</sup>Best overall response for a particular subject was the best observed disease response per RECIST v1.1. Responses were based on an assessment by the investigator. No confirmation of response (CR + PR) was needed. Overall response assessments occurring after onset of subsequent anticancer therapy were censored.

<sup>b</sup>Assessed every 8 weeks until Week 56. Results at Week 8 are presented.

**Figure 1.**

Summary of treatment duration with tumor response in the three cohorts. Cohort 1 (225 mg ARO-HIF2), Cohort 2 (525 mg ARO-HIF2), and Cohort 3 (1050 mg ARO-HIF2). Abbreviations: A, Subject A; B, Subject B; PD, progressive disease; PR, partial response; SD, stable disease.



## Discussion

HIF2 $\alpha$  is a key tumorigenic driver of ccRCC (7, 16, 23) and a first-in-class HIF2 $\alpha$  inhibitor has been recently approved by the FDA for the treatment of metastatic ccRCC. ARO-HIF2 is an siRNA therapeutic designed to target HIF2 $\alpha$  mRNA for degradation and interrupt further downstream pro-oncogenic gene activation in ccRCC. This Phase 1 study of ARO-HIF2 is the first clinical study using a tumor-targeted siRNA against HIF2 $\alpha$ . A total of 26 subjects with ccRCC were enrolled, 7 subjects in Cohort 1 (225 mg QW), 10 subjects in Cohort 2 (525 mg QW), and 9 subjects in Cohort 3 (1,050 mg QW).

PK values were generally comparable between the first and third weekly administration and pre-dose concentrations were very low, suggesting that accumulation of ARO-HIF2 in plasma is unlikely, even at the highest ARO-HIF2 dose (1,050 mg QW). About 99% of ARO-

HIF2 appeared to be cleared by tissues with minimal renal clearance. A higher than dose proportional exposure was observed, indicating PK nonlinearity. This may reflect how ARO-HIF2 is taken up by cells, specifically, it may illustrate receptor capacity limited tissue uptake.

There was a dose-dependent increase in ARO-HIF2 concentrations in tumor cells. Unexpectedly, there was a marked uptake in stromal cells, including endothelial cells. ARO-HIF2 concentrations in stromal cells were uniformly high and comparable with those achieved in tumor cells at the highest ARO-HIF2 dose (1,050 mg QW). Furthermore, although there was a dose-dependent (although not dose proportional) increase in ARO-HIF2 in tumor cells, concentrations in stromal cells were relatively constant across all dose levels. These data suggest that ARO-HIF2 is initially distributed to stromal cells before reaching tumor cells, which occurs once stromal cells are saturated.

**Figure 2.**

Waterfall plot of best sum of diameters percentage of change for target lesions. Among the 6 subjects with a percentage of change in target lesion size in the SD range (between -30% and +20%) who had PD, 4 subjects had PD of a non-target lesion, 1 subject had a new lesion, and 1 subject had both PD in a non-target lesion and a new lesion. Abbreviations: A, Subject A; B, Subject B; PD, progressive disease; PR, partial response; SD, stable disease.

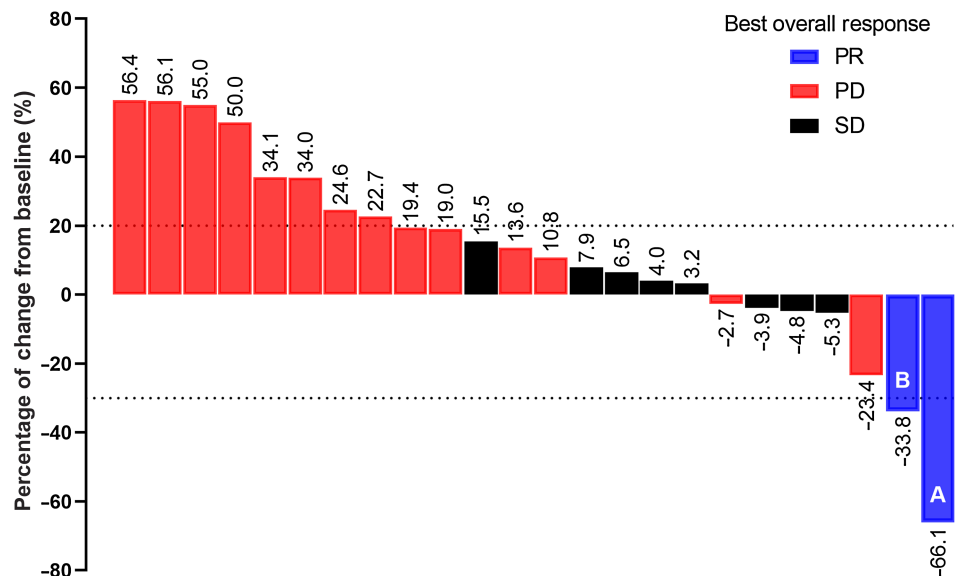


**Table 4.** Summary of key tumor characteristics and biomarkers for subjects who responded to therapy.

Subject ID (dose level)	Response	IHC ITGB3 H-score at screening (week 2)	VHL by NGS (variant frequency)	IHC HIF2 $\alpha$ H-score at screening (week 2)	HIF2 $\alpha$ mRNA <sup>a</sup> by RNAscope	HIF2 $\alpha$ mRNA <sup>a</sup> by qPCR	EPO level (IU/L) baseline →lowest post baseline	Hb level (g/dL) baseline →lowest post baseline
A (525 mg QW)	PR	10 (3)	In frame deletion (0.1231–0.3057)	270 (270)	33% reduction	24% reduction	208.1 → 50.4 <sup>b</sup>	12.0 → 9.3
B (1,050 mg QW)	PR	NA <sup>c</sup> (300)	No variants detected	NA <sup>c</sup> (230)	36% reduction	NA <sup>c</sup>	21.1 → 11.3	13.6 → 11.4

Abbreviations: EPO, erythropoietin; Hb, hemoglobin; ID, identification; IHC, immunohistochemistry; ITGB3 Integrin  $\alpha v \beta 3$ ; mRNA, messenger RNA; NA, not applicable; NGS, next-generation sequencing; PR, partial response; qPCR, quantitative polymerase chain reaction; QW, once weekly; SD, stable disease; VHL, von Hippel-Lindau gene.

<sup>a</sup>Change in HIF2 $\alpha$  mRNA in tumor from baseline to week 2.

<sup>b</sup>Subject A had paraneoplastic polycythemia.

<sup>c</sup>Insufficient tumor content (40% required for PCR, 5% required for IHC) in screen biopsy.

Assessing the impact of ARO-HIF2 on HIF2 $\alpha$  levels proved challenging, particularly with respect to protein levels. Although tumor biopsies collected at Week 2 generally showed a reduction in median HIF2 $\alpha$  mRNA (by RT-qPCR and RNAscope) a correlation was not observed between the level of knockdown and ARO-HIF2 dose. This was unexpected because a correlation was observed between dose and ARO-HIF2 uptake in tumor cells. We evaluated whether there was a correlation between the level of integrin  $\alpha v \beta 3$  expression on tumor cells and HIF2 $\alpha$  depletion, but no correlation was found. We also sought to determine whether there was a correlation between HIF2 $\alpha$  depletion and antitumor activity.

Two subjects responded to ARO-HIF2, achieving a PR [Subject A (Cohort 2, 525 mg) and Subject B (Cohort 3, 1,050 mg)]. Subject A, preliminarily reported in Ma and colleagues (10), was a 70-year-old female with metastatic ccRCC that had progressed on 2 prior VEGF-targeted therapies (sunitinib and axitinib) and an ICI (nivolumab). Tumor analyses showed an in-frame deletion of VHL and chromosome 3p loss. The subject had markedly elevated baseline EPO levels, resulting in paraneoplastic polycythemia requiring frequent phlebotomies to control RBC counts. Paraneoplastic polycythemia is most often associated with ccRCC and is likely driven by HIF2. The subject enrolled in Cohort 2 (525 mg QW) and biopsies after 2 doses of ARO-HIF2 showed HIF2 $\alpha$  mRNA downregulation in tumor cells (–24% by qPCR and –33% by RNAscope). In keeping with HIF2 $\alpha$  knockdown, EPO levels rapidly decreased from 208.1 IU/L to 50.4 IU/L (10). There were no notable changes in circulating VEGF levels, which were normal at baseline, an observation that is consistent with the notion that most plasma VEGF is produced by non-tumor cells in an HIF2-independent manner (16). The subject developed a hemorrhage from an intestinal metastasis, which resulted in an acute coronary syndrome leading to study discontinuation after 2 doses of ARO-HIF2. At Week 8 (off study), a PR was achieved with a 66% reduction in target lesion size. Notably, the response was maintained, and the subject remained off systemic therapy for approximately 5 months (10). This is particularly striking given that she had overt progression during the two week washout period prior to receiving the first dose of ARO-HIF2 requiring repeat scans (10). In addition, substantial antitumor activity was also observed in a tumor-graft line generated from one of the biopsy samples (10).

The second subject with a PR (Subject B) was a 49-year-old male with metastatic ccRCC that had progressed on VEGF directed (cabozantinib and lenvatinib) and ICI therapy (nivolumab, ipilimumab, and pembrolizumab). Although no VHL deletion was detected, VHL inactivation through gene methylation cannot be excluded. A 36%

reduction in HIF2 $\alpha$  mRNA by RNAscope was observed. Baseline EPO level (21.1 IU/L) was slightly above the normal range of 2.6 to 18.5 IU/L and fluctuated between 11.3 and 22.7 IU/L during the study. There were no notable changes in circulating VEGF. At Week 8, a PR was achieved with a 31% reduction in target lesion size, which was maintained at week 16 (33.8% reduction). The subject discontinued treatment after 15 doses of 1,050 mg ARO-HIF2 QW (day 132) due to Grade 2 peripheral neuropathy, which resolved. Notably, as for Subject A, the response was maintained after discontinuation of ARO-HIF2, and the subject remained off systemic therapy for an additional 7 months.

Overall, the response rate in this study was low, which may be due to several factors. First, subjects in Cohort 1 and perhaps to some extent in Cohort 2, may have received suboptimal doses of ARO-HIF2. Although pharmacodynamic data were inconclusive, an increase in ARO-HIF2 in tumor cells was observed with progressively higher doses. In addition, the responses observed were in Cohorts 2 and 3. Second, on the basis of the collective experience with HIF2 inhibitors in sporadic ccRCC, response rates are around 25% (20, 21). Third, effective HIF2 engagement by siRNA will depend on uptake by tumor cells, a process that is contingent on integrin receptor expression and some tumors may not express sufficient integrin levels. Thus, responses might have been expected in 10% to 15% of patients in an unselected population.

Notably, in Subjects A and B, tumor responses to ARO-HIF2 lasted for several months after ARO-HIF2 discontinuation, which suggests that ARO-HIF2 may remain in tumor cells for an extended period. This is in keeping with other siRNA drugs and suggests that ARO-HIF2 may not need to be administered QW.

It is unclear whether ARO-HIF2 induces anemia, which is an on-target adverse effect of HIF2 inhibitors, which downregulate EPO secretion by normal kidney cells. A reduction in hemoglobin was observed over time, but this may also result from tumor progression. To separate anemia induced by ARO-HIF2 from anemia of tumor progression, we focused on responding subjects. In Subject A with paraneoplastic polycythemia, EPO levels were downregulated to the normal range. In addition, EPO levels remained within the normal range in Subject B. Given that EPO levels did not drop below normal in these subjects where HIF2 $\alpha$  was downregulated in tumor cells, ARO-HIF2 may not be taken up by normal EPO producing cells in the kidney, which may lack the integrin receptor. Furthermore, although overall EPO levels trended down in study patients across the 3 cohorts, the downregulation was modest, and levels consistently remained

within the normal range in all patients. This is in contrast with belzutifan, which targets HIF2 $\alpha$  indiscriminately leading to EPO downregulation below the normal threshold (21).

Whether ARO-HIF2 is associated with hypoxia, a second on-target effect of HIF2 inhibitors, is unclear. In this study, there were 2 cases of treatment-related Grade 3 hypoxia, one in a subject with pneumonia and another in a subject with progressing lung metastases. The incidence of Grade  $\geq 3$  hypoxia was lower with ARO-HIF2 (7.7%) than with belzutifan (16%; ref. 21). However, some subjects may have been underdosed in this study. Nevertheless, the presence of pulmonary abnormalities in subjects with hypoxia in the current study offers a potential alternative explanation.

Six subjects (23.1%) treated with ARO-HIF2 developed neurotoxicity related to ARO-HIF2 (8 events) during the treatment window, including one TEAE of Grade 4 neuropathy peripheral (not recovered/not resolved). One Grade 3 chronic inflammatory demyelinating polyradiculoneuropathy (not recovered/not resolved) and one Grade 3 Guillain-Barré syndrome (recovered/resolved) also occurred off study. Although the mechanism remains unclear, similar toxicities have not been observed with belzutifan. High levels of ARO-HIF2 uptake by stroma cells suggest that although ARO-HIF2 may be directed to the tumor, ARO-HIF2 uptake by other cell types does occur. How ARO-HIF2 is causing neurotoxicity is unclear and while it seems unlikely, we cannot exclude off target effects of the RNAi trigger.

Oligonucleotide-based therapeutics are emerging as a new class of highly specific drugs and several RNA-targeted drugs have been approved by regulatory agencies for metabolic and other diseases (31). In the completed AROHIF21001 Phase 1 study with dose escalation, 2 subjects had PRs. These signs of target engagement and tumor reductions expand previous studies of human ccRCC transplants in mice (10) and provide proof of concept that siRNA can be used to target tumors in a specific manner. An added advantage of ARO-HIF2 is its activity against resistant mutant HIF2 $\alpha$ , which develops following PT drugs (10).

Limitations to the current study include most importantly a lack of robust pharmacodynamic data. Although preclinical models showed a correlation between HIF2 $\alpha$  knockdown and antitumor activity (10), this could not be assessed in subjects treated with ARO-HIF2. This likely reflects the increased complexity of drawing inferences from biopsy samples. This challenge precluded correlations between dose and target engagement as well as between target engagement and response. Another limitation relates to the number of biopsies. Specifically, a single post-treatment biopsy at a fixed interval would not have sufficed to determine the optimal treatment interval. Ultimately, difficulties from tissue-based pharmacodynamic assays may be overcome with imaging tools and current efforts are underway to measure HIF2 $\alpha$  in tumors in patients using a theranostic approach (NCT04989959). It is also worth noting that prolonged disease control in the 2 subjects with a response for several months after ARO-HIF2 discontinuation suggests that weekly administration of ARO-HIF2 may not be necessary. Whether reducing the dosing frequency would affect the toxicities observed, in particular neurotoxicity, is unknown.

In conclusion, we report the results of a first-in-human study of a representative population (Supplementary Table S7) using a tumor-directed siRNA (ARO-HIF2) against HIF2 $\alpha$ , a key driver of ccRCC. Overall, the study provides proof of concept for ligand-targeted oligonucleotide-based therapies in oncology. The protocol-defined MTD was not reached and a definitive RP2D and optimal administration schedule were not determined. Preliminary evidence of activity was observed; however, further development was hampered by off-

target toxicity. The potential of ARO-HIF2 could be improved by decreasing neuropathy, in addition to improving target engagement in tumor tissue.

## Authors' Disclosures

J. Brugarolas reports grants from Arrowhead Pharmaceuticals and NCI P50CA196516 during the conduct of the study, other support from Regeneron Pharmaceuticals, and personal fees from Telix Pharmaceuticals, Exelixis, Johnson & Johnson, and Eisai outside the submitted work; in addition, J. Brugarolas reports a US patent for 11,576,889-B2 methods of identifying and treating patients with HIF-2 inhibitor resistance issued to University of Texas Board of Regents, a patent for 17/206,895 biomarkers of response to HIF-2 inhibition in cancer and methods for the use thereof pending to University of Texas Board of Regents, and a patent for 17/153,128 PET radiopharmaceuticals for non-invasive evaluation of HIF-2 pending to University of Texas Board of Regents. K.E. Beckermann reports personal fees from Aveo, Aravive, alpine bioscience, BMS, Exelixis, Nimbus, Merck, Arcus, and Eisai and grants from Pionyr and ArsenalBio during the conduct of the study. B.I. Rini reports grants and personal fees from Merck, Pfizer, and BMS, grants from Arcus, and personal fees from Eisai outside the submitted work. E.T. Lam reports grants from Arrowhead Pharmaceuticals, Merck, Roche, Pfizer, BMS, and Exelixis during the conduct of the study. J. Hamilton reports other support from Arrowhead Pharmaceuticals during the conduct of the study and other support from Arrowhead Pharmaceuticals outside the submitted work. T. Schluep reports personal fees from Arrowhead Pharmaceuticals during the conduct of the study and personal fees from Arrowhead Pharmaceuticals outside the submitted work. M. Yi reports personal fees from Arrowhead Pharmaceuticals during the conduct of the study. S.C. Wong reports patents for WO2016/196239 pending, WO2019/210200 pending, WO2019/161213 pending, and WO2020/146521 pending and reports employment by and ownership of stock options of Arrowhead Pharmaceuticals. Z. Mao reports grants from Arrowhead Pharmaceuticals outside the submitted work. N. M. Tannir reports grants from Arrowhead Pharmaceuticals during the conduct of the study, grants and personal fees from Bristol Myers Squibb, Exelixis, and Nektar Therapeutics, grants from Calithera Biosciences and Novartis, and personal fees from AstraZeneca, Eisai Medical Research, Merck Sharp & Dohme, Intellisphere, and Oncorena outside the submitted work. No disclosures were reported by the other authors.

## Authors' Contributions

**J. Brugarolas:** Conceptualization, resources, formal analysis, supervision, validation, investigation, visualization, methodology, writing—original draft, project administration, writing—review and editing. **G. Obara:** Investigation, writing—review and editing. **K.E. Beckermann:** Investigation, writing—original draft, writing—review and editing. **B. Rini:** Investigation, writing—review and editing. **E.T. Lam:** Investigation, writing—review and editing. **J. Hamilton:** Conceptualization, data curation, supervision, funding acquisition, writing—review and editing. **T. Schluep:** Conceptualization, resources, data curation, funding acquisition, visualization, writing—original draft, project administration, writing—review and editing. **M. Yi:** Data curation, formal analysis, validation, visualization, writing—original draft, writing—review and editing. **S. Wong:** Data curation, validation, visualization, methodology, writing—original draft, writing—review and editing. **Z.L. Mao:** Investigation, writing—review and editing. **E. Gamelin:** Investigation, writing—review and editing. **N.M. Tannir:** Conceptualization, supervision, investigation, methodology, writing—original draft, writing—review and editing.

## Acknowledgments

We thank the patients who participated in the study and their families. We thank Andrea Clark, Aroga Biosciences, for editorial assistance. This study was sponsored by Arrowhead Pharmaceuticals, Inc. J. Brugarolas is supported by P50CA196516. This article is written in memoriam of our esteemed colleague Dr. N.J. Vogelzang, Comprehensive Cancer Centers of Nevada, and his contributions to the conduct of the study.

## Note

Supplementary data for this article are available at Clinical Cancer Research Online (<http://clincancerres.aacrjournals.org/>).

Received October 3, 2023; revised February 9, 2024; accepted March 26, 2024; published first April 23, 2024.

## References

- Kaelin WG Jr. The von Hippel-Lindau tumor-suppressor protein and clear cell renal carcinoma. *Clin Cancer Res* 2007;13:680s–4s.
- Schodel J, Grampp S, Maher ER, Moch H, Ratcliffe PJ, Russo P., et al., Hypoxia-inducible transcription factors, and renal cancer. *Eur Urol* 2016;69:646–57.
- Shen C, Kaelin WG Jr. The VHL/HIF axis in clear cell renal carcinoma. *Semin Cancer Biol* 2013;23:18–25.
- Linehan WM, Ricketts CJ. The Cancer Genome Atlas of renal cell carcinoma: findings and clinical implications. *Nat Rev Urol* 2019;16:539–52.
- Nickerson ML, Jaeger E, Shi Y, Durocher JA, Mahurkar S, Zaridze D, et al. Improved identification of von Hippel-Lindau gene alterations in clear cell renal tumors. *Clin Cancer Res* 2008;14:4726–34.
- Gordan JD, Bertout JA, Hu CJ, Diehl JA, Simon MC. HIF-2alpha promotes hypoxic cell proliferation by enhancing c-myc transcriptional activity. *Cancer Cell* 2007;11:335–47.
- Kondo K, Kim WY, Lechpammer M, Kaelin WG Jr. Inhibition of HIF2alpha is sufficient to suppress pVHL-defective tumor growth. *PLoS Biol* 2003;1:E83.
- Raval RR, Lau KW, Tran MG, Sowter HM, Mandriota SJ, Li JL, et al. Contrasting properties of hypoxia-inducible factor 1 (HIF-1) and HIF-2 in von Hippel-Lindau-associated renal cell carcinoma. *Mol Cell Biol* 2005;25:5675–86.
- Dengler VL, Galbraith M, Espinosa JM. Transcriptional regulation by hypoxia-inducible factors. *Crit Rev Biochem Mol Biol* 2014;49:1–15.
- Ma Y, Joyce A, Brandenburg O, Saatchi F, Stevens C, Toffessi Tcheuyap V, et al. HIF2 inactivation and tumor suppression with a tumor-directed RNA-silencing drug in mice and humans. *Clin Cancer Res* 2022;28:5405–18.
- Ferrara N, Hillan KJ, Gerber HP, Novotny W. Discovery and development of bevacizumab, an anti-VEGF antibody for treating cancer. *Nat Rev Drug Discov* 2004;3:391–400.
- Choueiri TK, Motzer RJ. Systemic therapy for metastatic renal-cell carcinoma. *N Engl J Med* 2017;376:354–66.
- Covello KL, Kehler J, Yu H, Gordan JD, Arsham AM, Hu CJ, et al. HIF-2alpha regulates Oct-4: effects of hypoxia on stem cell function, embryonic development, and tumor growth. *Genes Dev* 2006;20:557–70.
- Hoefflin R, Harlander S, Schafer S, Metzger P, Kuo F, Schonenberger D, et al. HIF-1alpha and HIF-2alpha differently regulate tumour development and inflammation of clear cell renal cell carcinoma in mice. *Nat Commun* 2020;11:4111.
- Scheuermann TH, Li Q, Ma HW, Key J, Zhang L, Chen R, et al. Allosteric inhibition of hypoxia-inducible factor-2 with small molecules. *Nat Chem Biol* 2013;9:271–6.
- Chen W, Hill H, Christie A, Kim MS, Holloman E., Pavia-Jimenez A, et al. Targeting renal cell carcinoma with a HIF-2 antagonist. *Nature* 2016;539:112–7.
- Cho H, Kaelin WG. Targeting HIF2 in clear cell renal cell carcinoma. *Cold Spring Harb Symp Quant Biol* 2016;81:113–21.
- Wallace EM, Rizzi JP, Han G, Wehn PM, Cao Z, Du X, et al. A small-molecule antagonist of HIF2alpha is efficacious in preclinical models of renal cell carcinoma. *Cancer Res* 2016;76:5491–500.
- Xu R, Wang K, Rizzi JP, Huang H, Grina JA, Schlachter ST, et al. 3-[(1S,2S,3R)-2,3-Difluoro-1-hydroxy-7-methylsulfonylindan-4-yl]oxy-5-fluorobenzonitrile (PT2977), a hypoxia-inducible factor 2alpha (HIF-2alpha) inhibitor for the treatment of clear cell renal cell carcinoma. *J Med Chem* 2019;62:6876–93.
- Courtney KD, Infante JR, Lam ET, Figlin RA, Rini BI, Brugarolas J, et al. Phase I dose-escalation trial of PT2385, a first-in-class hypoxia-inducible factor-2alpha antagonist in patients with previously treated advanced clear cell renal cell carcinoma. *J Clin Oncol* 2018;36:867–74.
- Choueiri TK, Bauer TM, Papadopoulos KP, Plimack ER, Merchan JR, McDermott DF, et al. Inhibition of hypoxia-inducible factor-2alpha in renal cell carcinoma with belzutifan: a phase 1 trial and biomarker analysis. *Nat Med* 2021;27:802–5.
- Jonasch E, Donskov F, Iliopoulos O, Rathmell WK, Narayan VK, Maughan BL, et al. Belzutifan for renal cell carcinoma in von Hippel-Lindau disease. *N Engl J Med* 2021;385:2036–46.
- Courtney KD, Ma Y, Diaz de Leon A, Christie A, Xie Z, Woolford L, et al. HIF-2 complex dissociation, target inhibition, and acquired resistance with PT2385, a first-in-Class HIF-2 inhibitor, in patients with clear cell renal cell carcinoma. *Clin Cancer Res* 2020;26:793–803.
- Fire A, Xu S, Montgomery MK, Kostas SA, Driver SE, Mello CC. Potent and specific genetic interference by double-stranded RNA in *Caenorhabditis elegans*. *Nature* 1998;391:806–11.
- Sharp PA. RNA interference—2001. *Genes Dev* 2001;15:485–90.
- Vogetseder A, Thies S, Ingold B, Roth P, Weller M, Schraml P, et al. alpha-Integrin isoform expression in primary human tumors and brain metastases. *Int J Cancer* 2013;133:2362–71.
- Desgrosellier JS, Cheresh DA. Integrins in cancer: biological implications and therapeutic opportunities. *Nat Rev Cancer* 2010;10:9–22.
- Wong SC, Cheng W, Hamilton H, Nicholas AL, Wakefield DH, Almeida A, et al. HIF2alpha-targeted RNAi therapeutic inhibits clear cell renal cell carcinoma. *Mol Cancer Ther* 2018;17:140–9.
- Wong SC, Nicholas A, Carlson JC, Shu D, Liu C, Chu R, et al. Optimizing the potency and dosing design for ARO-HIF2: an RNAi therapeutic for clear cell renal cell carcinoma [abstract]. In: Proceedings of the American Association for Cancer Research Annual Meeting 2019; 2019 Mar 29-Apr 3; Atlanta, GA. Philadelphia (PA): AACR; Cancer Res 2019;79(13 Suppl):Abstract nr 4775.
- Wang L, Ji C. Advances in quantitative bioanalysis of oligonucleotide biomarkers and therapeutics. *Bioanalysis* 2016;8:143–55.
- Zhang MM, Bahal R, Rasmussen TP, Manautou JE, Zhong XB. The growth of siRNA-based therapeutics: updated clinical studies. *Biochem Pharmacol* 2021;189:114432.